Numerical and Experimental Computations of Pavement Surface Effects on Rolling Resistance

Dmytro A. Mansura, Nicholas H. Thom and Hartmut J. Beckedahl

BACKGROUND

Air pollution, limited finite fossil fuel and increased price of fuel push tyre and pavement researchers to find ways to produce the tyres and pavements as sustainably and cost-effectively as modern technologies allow. Conventional means to achieve minimal fuel consumption are to improve aerodynamics, transmission and tyre characteristics; pavements are now seen as a further approach to lowering the energy consumption. It has long been known that pavements affect fuel use, just as tyres do, through rolling resistance (RR), and that decreasing RR by 10 % typically saves 1-4 % of fuel (*1*). To overcome RR a typical car on average consumes 119 litres of fuel annually due to both vehicle and pavement factors. RR consists of both compressive and tangential energy loss mechanisms (comprising tyre macro-distortion, tyre micro-distortion and pavement macro-distortion), causing the leading part of the contact area to be more heavily compressed than the trailing part, and it varies in magnitude from 25 N to 80 N per car tyre (*2*).

The energy being dissipated in the pavement is tied with wave propagation along, across and inside the road structure that causes asymmetry in the deflection bowl under the tyre. Recent computations (*3*) have shown that the stiffness of the uppermost pavement layer is much more significant than those of underlying layers, meaning that a stiffer upper pavement saves energy. The other two losses take place within the tyre. The occurrence of macro-distortional energy loss is a function of compressive, tangential (micro-slippage and shear-induced inertia) and wave-induced inertial deformations. Additionally, pavement texture indentations into the visco-elastic tread compound induce micro-distortional energy loss. These contact distortions give rise to local compression which includes a visco-elastic and to a smaller extent inertial component that influence the moment balance in the tyre-pavement contact patch, but a true quantitative understanding is still lacking.

A prime element of this study was therefore to develop a simplified and computationally efficient numerical multi-scale method for prediction of micro-distortional RR in order to analyse the effects of pavement macro-texture (0.5 mm-50 mm) with various shapes, sizes and packing arrangements. Numerical RR predictions have then been qualitatively confirmed and approximately adjusted for real-life surfaces based on laboratory testing since traditional tests are unable to isolate the texture-dependent contributions to RR. In the long-term, this methodology could supplement Life-Cycle Assessment (LCA) tools and be applied for optimisation of road texture to minimise RR without sacrificing drainage and skid resistance functionality.

NUMERICAL ANALYSIS

A 3-D numerical multi-scale model comprising both macro-scale (whole slick radial tyre) and micro-scale (tread-stone contact) elements, has been implemented in ABAQUS. The macro-scale steady-state analysis was based on a 175 SR14 Yokohama tyre taken from ABAQUS open

source documentation (*4*). The modelling of steady-state rolling was constructed from a sequence of static and brake/traction simulations, all of which were conducted applying ABAQUS/Implicit (Standard). This analysis enabled derivation of loading, holding and unloading rates (Figure 1) to be applied to an idealized stone indenter at the micro-scale model, as well as generating macro-distortional RR. In this analysis the tyre was loaded to 3300 N and inflated to a pressure of 200 kPa. Friction was represented by Coloumb's law.

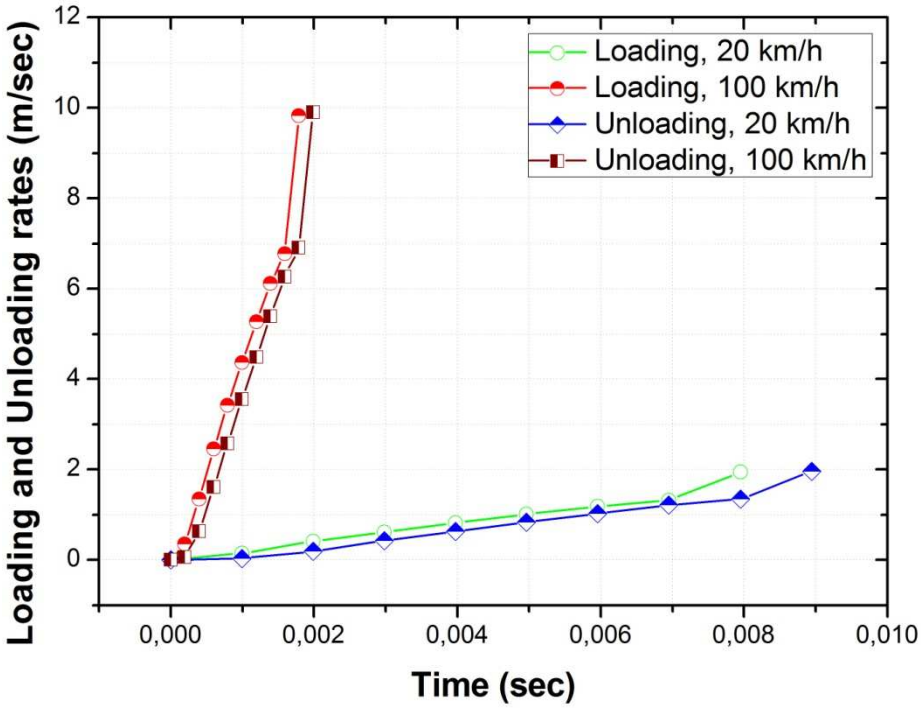

Figure 1 Loading and unloading rates for 20 km/h and 100 km/h under 3300 N tyre loading and 0.7 coefficient of friction, derived from tyre FE model

By ensuring a near-zero moment balance state about the tyre axis using a trial and error technique, simulation of the free-rolling condition was achieved. An efficient runtime and converged solution were possible by using a finer mesh in the contact area covering 40° of arc and a coarser mesh covering the remaining 320°. In both models visco-elastic rubber properties were described by a series of rheological Maxwell elements (Prony series) corresponding to a typical tyre temperature of 55ºC, where elastic and viscous responses are captured by, respectively, springs and dashpots. The computations of macro-distortional RR agreed reasonably with the results found in the literature for the same tyre type (*5*).

The micro-scale model was made up of a homogeneous visco-elastic 45x45 mm tread block (i.e. a piece of a tyre surface) and a rigid stone (Figure 2) and generated by application of ABAQUS/Explicit to deduce micro-distortional RR based on contact forces and stone indentations (*6*).

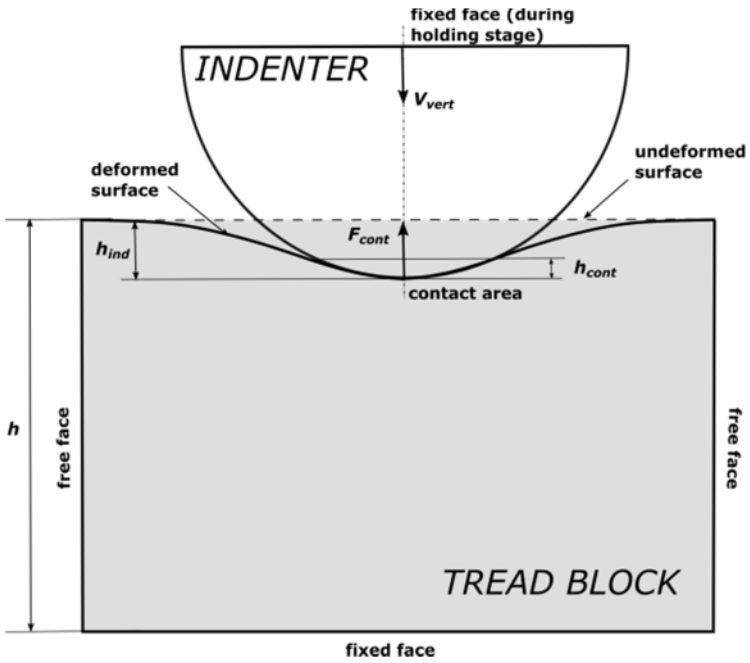

Figure 2 A schematic configuration of the FE tread-stone contact simulation with boundary conditions

The model takes account of three interaction phases, namely indentation/loading of the stone into the tread rubber, holding and release/unloading. The block was fixed, while the stone/indenter indented vertically into the rubber. Stone boundary conditions were prescribed in terms of vertical velocity, which was outputted from the macro-scale model for a set of centrally located nodes before and after the velocity became zero in the contact patch. These loading/unloading rates corresponded to a given indentation, related to 3300 N tyre load and 200 kPa inflation pressure. As a result of compound viscosity and inertia, the loading rates were found to be larger than the unloading rates (Figure 2).

A hypothetical asphalt mixture is assumed to consist of a single-sized gradation making all surface stones identical. In this way, both smooth and rough pavements could be assessed by controlling the spacing between asperities along and across the contact. This discrete texture pattern was idealised in terms of hemispheres and cylinders, whereas concrete texture was represented by a pair of cuboid-shaped strips. The analysis of energy losses from bituminous surfaces was carried out with a single indenter, since the results were found to differ negligibly compared to the scenario with nine stones penetrating the tread. Furthermore, numerical simulations showed that the distribution of contact forces for an artificial indenter follows the trend and interaction phases induced by a real asperity with an angular shape.

Selection of an optimised three-layer mesh, with a finer mesh in the top layer as shown in Figure 3, and use of mass scaling by a factor of 4 gave a good compromise between accuracy and computational runtime. The model was discretised with linear brick C3D8R elements with reduced integration, hourglass and distortion control. A coarser mesh and increased mass scaling were found to cause significant oscillations in comparison with a finer mesh and zero mass scaling, respectively. In addition, an optimised contact stiffness level was included to avoid numerical instability at tread-indenter interface.

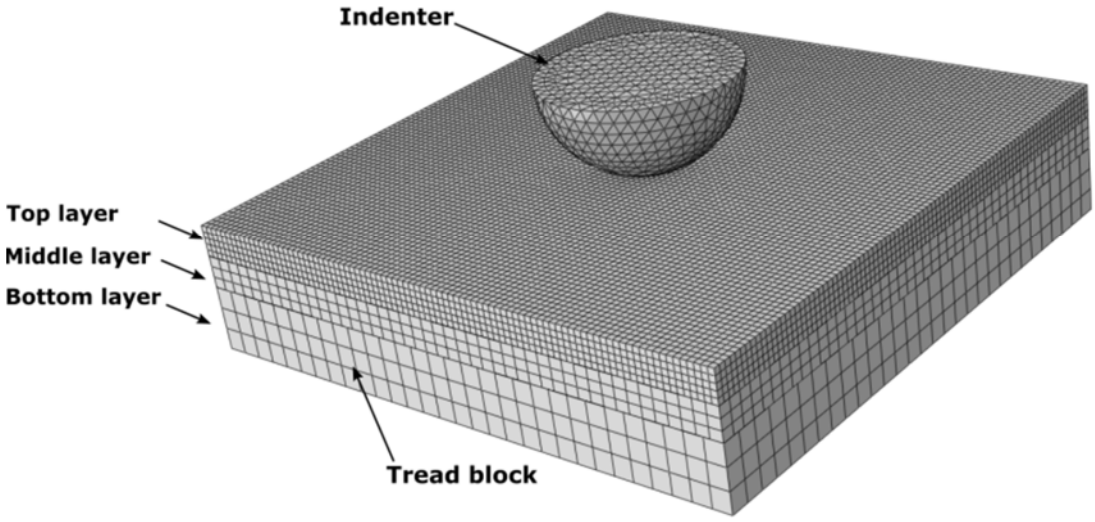

Figure 3 A FE tread-stone analysis with a hemispherical indenter in contact

To predict micro-distortional energy loss per tyre, the energy loss for a single stone was quantified from contact forces and indentations for a given loading; this loss was then scaled to give a value for the whole tyre. The results from this method approximated more closely the influences of protruding texture on RR as compared with values generated by the moment-based method described in (*6*). Evaluation of different texture packing arrangements was made by varying the spacing between asperities along and across the contact enabling both rough and smooth surfaces to be studied.

EXPERIMENTAL ANALYSIS

Adjustment and qualitative confirmation of numerical micro-distortional RR were carried out based on the so-called ‘packed indenters loading test’ (PILT) using an Instron 8801 servo-hydraulic machine under load control. Both cored samples (Stone Mastic Asphalt-SMA and Hot Rolled Asphalt-HRA) and idealised packed spherical surfaces were examined using this test. In the PILT test a specimen is put onto a base platform and on top of it a tread pad is placed with the tread pattern facing downwards (Figure 4). The test was run at the ambient room temperature of 20°, subjecting the specimen to 50 sinusoidal loads at a rate of 20 Hz.

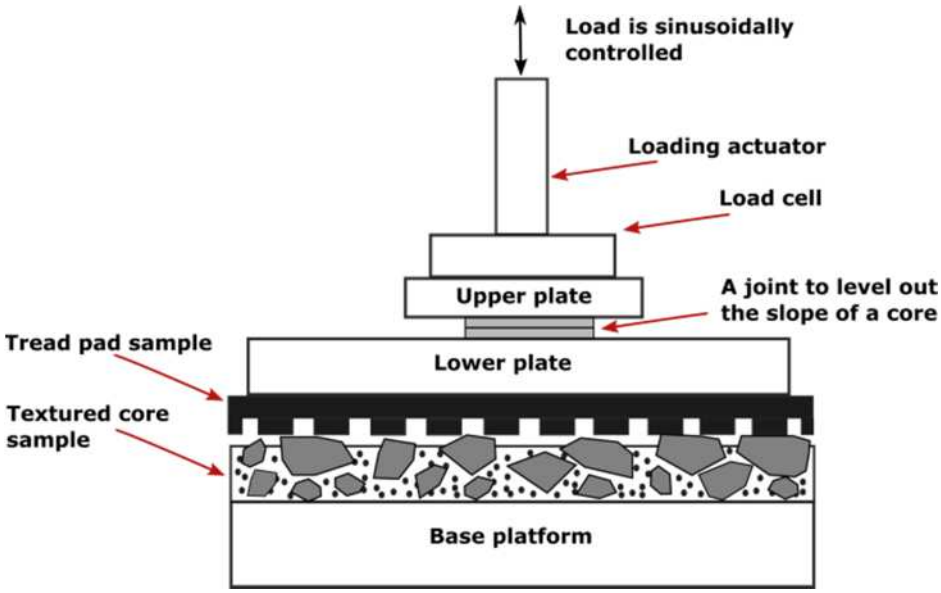

Figure 4 A schematic arrangement of the PILT set-up

The energy lost per pad during the 25th cycle was subsequently determined for a range of tread pads, surfaces and loading levels. This methodology then allowed micro-distortional RR per tyre to be calculated by multiplying the computed lost energy per pad by the number of pads in one metre. Comparing the FE calculations with the PILT results showed qualitative agreement; both the micro-distortional RR and stone indentations increased as a result of increased stone spacing.

To convert computed energy dissipation for spherical indenters to that for conventional paved surfaces, a calibration factor was determined, namely the average ratio between the energy lost over a realistic surface to that over an idealised surface. Further details on the experiment can be found in (*6*).

RESULTS and DISCUSSION

Figure 5 shows a typical contact compressive force distribution computed by the tread block-stone contact model. It was found that irrespective of the indenter shape and size, compressive forces undergo three interaction phases: the peak normal force at the end of the indentation/loading phase, followed by a gradual relaxation of the rubber compound until the start of unloading phase where the indenter releases from the tread surface. These were qualitatively corroborated by the results from other simulations (*7*). It was noted that due to the frequency-dependent behaviour of the rubber compound, a higher loading rate (100 km/h) increased the magnitude of the normal force as compared to a lower loading rate (20 km/h) by approximately 13 % both hemispherical and cylindrical indenters.

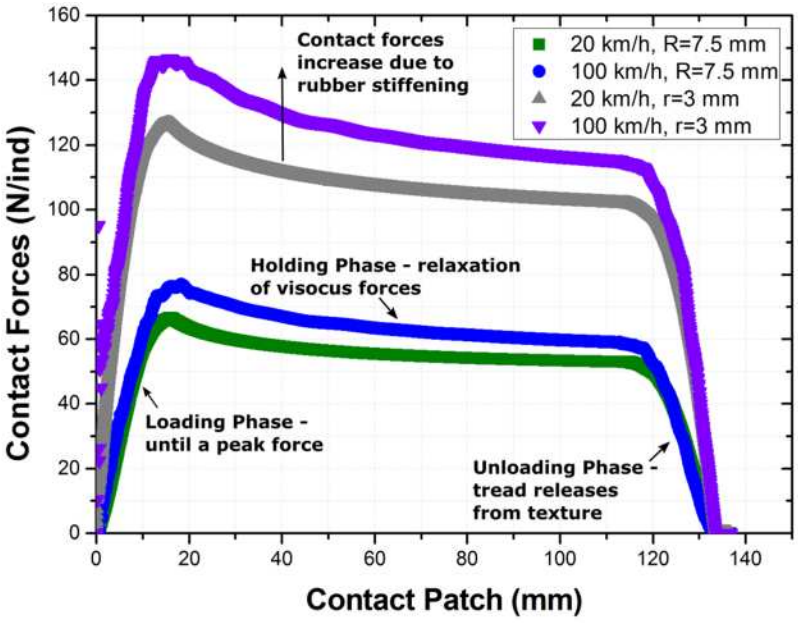

Figure 5 Contact force distribution along the contact patch in contact with a hemisphere of 7.5 mm radius and a cylinder of 3 mm radius at 1 mm indentation for 20 km/h and 100 km/h

The effect of numerical and physical noise on the normal forces appeared in the form of ripples at the end of the loading phase and during the holding phase as is seen in Figure 5. These relate to stiffening of the rubber, vibration of the tread block, mass scaling and reflective shock waves within the block. More pronounced effects were observed when a concrete surface (i.e. strips) was in contact, with initial spikes in the contact force.

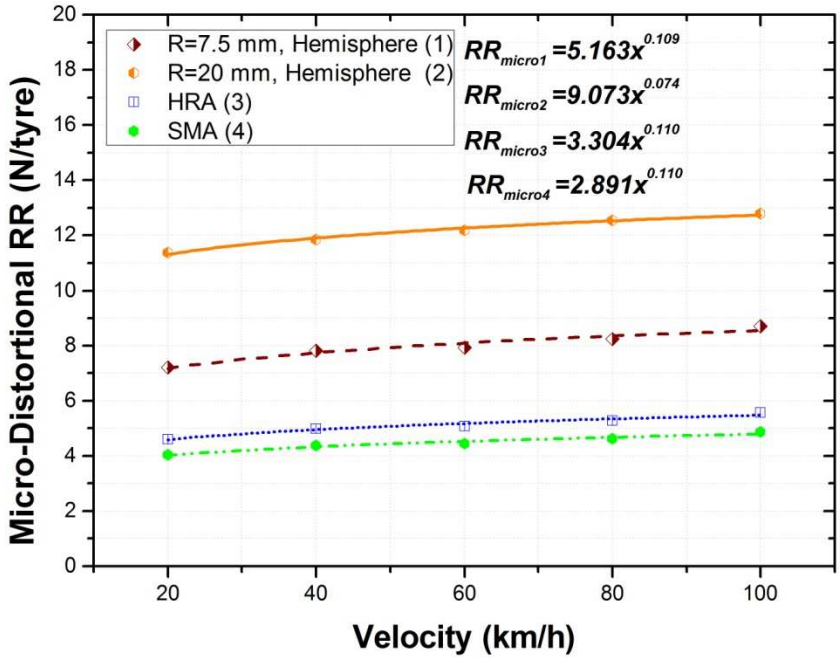

Figure 6 Micro-distortional RR as a function of velocity for hemispheres, HRA and SMA surfaces

The relationships between micro-distortional RR and velocity for various real and idealised surfaces are presented in Figures 6 and 7 for the chosen tyre under 3300 N loading. It may be

seen that micro-distortional energy loss approximately follows a power law for hemispheres and concrete texture with longitudinal and lateral configurations and strip widths of 15 and 19 mm. The linear increase shown for lateral concrete texture at a 5 mm strip width is simply because only two speeds were modelled.

For concrete texture the micro-distortional RR increased with respect to velocity, but in a relatively insensitive way, causing about 1.6-4 % increase for the combination of strips/grooves analysed. In contrast, cylindrical textures led to a parabolic relationship between micro-distortional RR and velocity with minimum values at around 60 km/h. Physically, this can be explained by the flat-ended shape of the cylinder which distorts the visco-elastic material, counteracting the stiffening of the rubber. Calculations indicated that the most environmentally friendly texture (i.e. least energy loss) was the longitudinally orientated concrete surface, inducing 0.18 N/tyre RR (Figure 7). This is reasonable since each strip distributes a larger force giving rise to a smaller compression into the tread.

In general, the micro-distortional RR for concrete texture, cylinders and fine hemispheres (i.e. 1 mm radius) stood at 1 N/tyre on average and was lower than that for coarser hemispheres. Further, by adjusting computed micro-distortional RR using the PILT-based adjustment factors to that of real life surfaces, it was confirmed that the rougher/looser surface of HRA results in more energy loss as compared to the smoother/tighter surface of SMA (Figure 6). The micro-distortional RR for these surfaces amounted to about 10 % of the total RR. Overall, both the experimental and the numerical predictions qualitatively agreed that the coarser surface causes more energy loss than the finer surface.

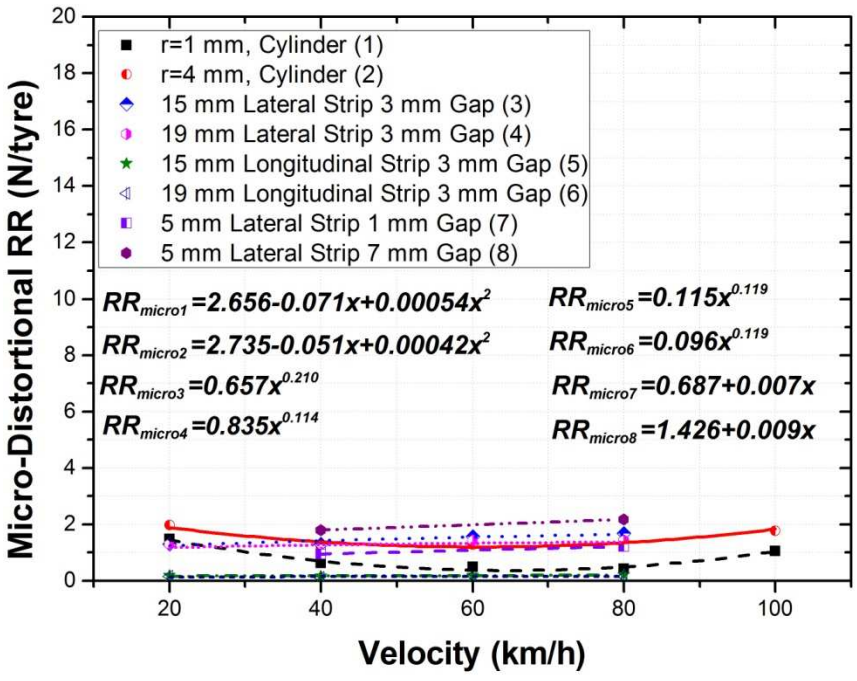

Figure 7 Micro-distortional RR as a function of velocity for cylindrical and concrete surfaces

CONCLUSIONS

Numerical 3-D multi-scale modelling and experiments have been developed for possible inclusion into LCA, allowing computation of texture-related RR during pavement service life. The effect of texture size was shown to be considerable, increasing the losses by a factor of 3.9 (from 1 mm radius to 20 mm radius) and 1.9 (from 1 mm radius to 4 mm radius) for hemispherical and cylindrical textures, respectively. A rougher/sparser texture packing affected RR adversely compared to a smoother/tighter option. The study showed that the most energy efficient surface was the longitudinally grooved concrete pattern. It was also found that a rise in the velocity increases lost energy. Further research should address energy losses for truck tyres, cover a broader range of realistic surfaces and examine speed scenarios beyond 100 km/h to take standing waves into account.

REFERENCES

1. Tires and Passenger Vehicle Fuel Economy. *Transportation Research Board Special Report 286*, National Research Council of the National Academies, Washington, D.C., 2006
2. Holmberg, K., Andersson, P., and Erdemir, A., "Global Energy Consumption Due to Friction in Passenger Cars", Tribology International, Vol. 47, 2012, pp. 221-234
3. Lu, T. The Influence of Pavement Stiffness on Vehicle Fuel Consumption. *PhD thesis*, University of Nottingham, UK, 2010
4. *ABAQUS On-line Documentation*. Dassault Systèmes, Providence, RI, USA
5. Behnke, R., and Kaliske, M. (2013). Computation of Energy Dissipation in Visco-Elastic Materials at Finite Deformation. *Proceedings of Applied Math. Mech.*, Vol. 13, pp. 159-160
6. Mansura, D. *Contributions of Pavement Texture Factors on Fuel Consumption*, Schriftenreihe des Fachzentrums Verkehr, Bd. 15. Aachen:Shaker (under preparation)
7. Liu, S., Sutcliffe, M., and Graham, W. (2012). Prediction of Tread Block Forces For a Free-Rolling Tyre in Contact with a Rough Road. *Wear*, Vol. 282-283, pp.1-11